Supplemental Information for "Cenozoic boron isotope variations in benthic foraminifers"

by

Markus Raitzsch and Bärbel Hönisch

1. MATERIALS AND METHODS

Eight ODP/DSDP sites in the subtropical to tropical Atlantic and Pacific Oceans were selected (Fig. DR1 and Table DR1), covering the past 50 My. For boron isotope analysis, 7 to 30 well-preserved monospecific shells (equivalent to 0.3 to 1.6 mg of $CaCO_3$, depending on shell size and abundance) of benthic foraminifers including *Planulina wuellerstorfi*, *Cibicidoides mundulus*, *Oridorsalis umbonatus*, and *Nutallides truempyi* were picked. The shells were crushed and cleaned according to established trace metal cleaning procedures (Barker et al., 2003), and finally dissolved in quartz-distilled 2 N HCl to yield sample solutions with approximately 1 ng B/µl. Up to eight 1-µl aliquots of the dissolved sample were loaded onto outgassed, zone-refined rhenium filaments, 1 µl of boron-free seawater was added to promote ionization, and analyses were done at 980-1020°C on a Thermal Ionization Mass Spectrometer (Thermo Scientific TRITON) at LDEO. This temperature difference has no discernible effect on the isotope ratio but few sample loads did not ionize sufficiently (i.e. <100 mV) at 980°C. Only data that showed less than 1‰ mass fractionation over the entire acquisition time (~30 min) were accepted and standardized against SRM NIST 951 boric acid standard. Reported $\delta^{11}B_c$ of each sample is typically based on at least three acceptable analyses, but in a few cases of very small samples only two acceptable measurements could be collected. The data of such a sample were only accepted and interpreted when another foraminifer species from the same sample was analyzed. Standard errors reported here are two external errors based on repeat measurements of an in-house consistency standard or two internal errors of repeat analyses of individual sample solutions, if that was larger than the external reproducibility. Two standard errors (2 s.e.) range between 0.28 and 0.69‰ and average 0.38‰ (Table DR1).

2. SPECIES-SPECIFIC δ^{11}B-OFFSETS

As there are specific offsets between the boron isotopic signatures of different benthic foraminifer species (Hönisch et al., 2008, Rae et al., 2011), we carried out cross-calibrations of co-existing species in samples and intervals where more than one of the four foraminifer species were available in sufficient abundance (Fig. 1C). This approach allowed us to normalize $\delta^{11}B_c$ from different species to the $\delta^{11}B_c$ of *P. wuellerstorfi*, which has been calibrated for $\delta^{11}B_c$ in

modern coretop sediments (Hönisch et al., 2008, Rae et al. 2011). Based on our cross-calibration studies we determined a negligible $\delta^{11}B_c$ difference of ~–0.19 ± 0.41‰ (±2 s.e.) between *P. wuellerstorfi* and *C. mundulus* in both the Atlantic and Pacific, whereas the average offset between *P. wuellerstorfi* and *O. umbonatus* is –1.41 ± 0.60‰ in the Atlantic and –0.84 ± 0.69‰ in the Pacific. This large difference between *O. umbonatus* specimens grown in the two ocean basins is likely related to the fact that this species lives infaunally within the upper centimeters of sediment (Rathburn and Corliss, 1994), where degradation of organic matter and carbonate dissolution modify pore-water pH and $\delta^{11}B_{pw}$ from the overlying bottom water (Rae et al., 2011). In contrast, *P. wuellerstorfi* is an epifaunal species that prefers an elevated habitat above the sediment-water interface (Lutze and Thiel, 1989) and is unaffected by pore-water deviations. Hence we applied ocean-specific offsets for normalizing $\delta^{11}B_c$ of *O. umbonatus* to *P. wuellerstorfi*. *Cibicidoides mundulus* is widely considered epifaunal, but may live within the uppermost centimeter within the sediment (Rathburn and Corliss, 1994). The isotopic and chemical composition, however, including $\delta^{11}B_c$ (Rae et al., 2011) and U/Ca (Raitzsch et al., 2011) is very similar to that of *P. wuellerstorfi*, suggesting that *C. mundulus* similarly calcifies close to bottom-water conditions. *Nuttalides truempyi* is an extinct species and a difference of 0.76 ± 0.48‰ has been applied to normalize $\delta^{11}B_c$ of *N. truempyi* to *P. wuellerstorfi* for the three oldest intervals in the Atlantic. This offset was derived from an independent and yet-to-be-published PETM study by B. Hönisch et al. (ODP 1263A: *N. truempyi*: 15.60 ± 0.10‰, *C. praemundulus*: 14.58 ± 0.27‰; 1263D: *N. truempyi*: 15.99 ± 0.83‰, *C. praemundulus*: 15.09 ± 0.48‰), assuming that the chemical composition of *C. praemundulus* is similar to *C. mundulus*, because it is its ancestor. The (propagated) uncertainty of normalized $\delta^{11}B_c$ is reported as the square root of the sum of squared two standard errors (2 s.e.) resulting from both the monospecific analyses and the cross-calibrations.

3. CALCULATING THE BORON ISOTOPIC COMPOSITION OF SEAWATER

Because the distribution of boron and its isotopes in the ocean is conservative (Foster et al., 2010), the benthic $\delta^{11}B_c$ record can be scaled to $\delta^{11}B_{sw}$ using the following equation:

$$\delta^{11}B_{sw} = \frac{10^{(-pH+pK_B)} * (-\alpha * \delta^{11}B_c + a * \alpha - \varepsilon) - \delta^{11}B_c + a}{-1 - 10^{(-pH+pK_B)}}$$

where pH is based on the total scale, pK_B is the equilibrium constant for the dissociation of $B(OH)_3$ (dependent on temperature, pressure, and salinity), α the fractionation factor, ε the isotopic fractionation ((α–1)*1000), and a the species-specific $\delta^{11}B_c$ offset from $\delta^{11}B_{borate}$, where the offset depends on the reference borate curve: Although the aqueous boron isotope fractionation of ε=27.2‰ (at 25°C) has been determined experimentally (Klochko et al., 2006),

and $\delta^{11}B$ recorded by various epibenthic foraminifera species is consistent with (Rae et al., 2011) or falls close (Hönisch et al., 2008) to the corresponding $\delta^{11}B$ of borate in seawater (Fig. DR3), uncertainties remain as to whether epibenthic $\delta^{11}B$ reflects $\delta^{11}B$ of borate in detail. It is clear that $\delta^{11}B$ values determined by NTIMS and MC-ICP-MS differ in absolute terms but irrespective of the technique used for $\delta^{11}B$ measurements, the slopes and inflexion points of all $\delta^{11}B_c$/pH calibration curves established to date over a wide pH-range are parallel to each other and show a less sensitive $\delta^{11}B$/pH relationship than expected from aqueous predictions alone (e.g., Hönisch et al., 2007; Krief et al., 2010; Rollion-Bard and Erez, 2010). The apparent isotopic fractionation recorded by marine carbonates is ε_{app}~20‰ (at 25°C) instead of the 27.2‰ determined experimentally (Klochko et al., 2006). Whereas the bulk shell $\delta^{11}B_c$ of shallow benthic foraminifers calibrated in the laboratory (Rollion-Bard and Erez, 2010) follows the same low $\delta^{11}B$ vs. pH sensitivity as observed in other marine carbonates (Hönisch et al., 2007; Krief et al. 2010), deep-sea benthic foraminifers have not yet been calibrated over a wide pH-range in the laboratory, and the small pH-variations in the deep ocean do not allow for determination of the slope. This problem was discussed by Hönisch et al. (2008) but we demonstrate that the same problem remains for the ICP-MS analyses of Rae et al. (2011), where 20 and 27.2‰ fractionation yield essentially identical fits between measured epibenthic and estimated bottom water $\delta^{11}B$-borate values (Fig. DR3). Due to this uncertainty we distinguish between aqueous (Klochko et al., 2006) and apparent sensitivity of $\delta^{11}B_c$ to pH based on empirical carbonate calibrations (Hönisch et al., 2007), and estimate $\delta^{11}B_{sw\text{-}inf}$ applying both constraints (Fig. 2). Consequently, the applied offsets a for *P. wuellerstorfi* are 0.7‰ and –5.4‰ for ε=27.2‰ and ε_{app}=20.0‰, respectively.

To approximate paleo-pK_B values, we applied the deep-sea temperature record from van Tuyll et al. (2007), which is in good agreement with the oxygen isotope temperature estimates for an ice-free world prior to 35 Ma (Zachos et al., 2001) and with benthic foraminifer Mg/Ca temperatures between 0 and 25 Ma (Lear et al., 2000). Salinity in turn was kept constant at 35‰, and hydrographic pressure was adjusted to paleodepths (Fig. DR4A). In order to test the influence of uncertainties afflicted with temperature, salinity and the surface-to-depth pH gradient estimates on $\delta^{11}B_{sw\text{-}inf}$, we assumed uncertainties of ±2°C for temperature, ±1 psu for salinity, and ±25% (= ±0.075) for the surface-to-deep pH gradient. The results show that the errors of calculated $\delta^{11}B_{sw\text{-}inf}$ due to temperature and salinity uncertainties are relatively low with ±0.12‰ and ±0.03‰, respectively, compared to the uncertainty in surface-to-depth pH gradient that accounts for about ±0.35‰ (Fig. 2). Consequently, the maximum error of $\delta^{11}B_{sw\text{-}inf}$ afflicted with temperature, salinity and pH gradient uncertainties is ±0.5‰, which is within the range of 2 standard errors resulting from analytical and cross-calibration uncertainties (Fig. 2).

The largest element of uncertainty in estimating past $\delta^{11}B_{sw}$ with this approach is given by potential long-term variations in deep-sea pH, which has likely changed throughout the Cenozoic. This parameter is afflicted with uncertainty, but because long-term variations in atmospheric pCO_2 and terrestrial weathering translate to ocean pH- and alkalinity-changes with relatively little time lag (at least compared to these million-year time scales), past surface and deep ocean pH should have covaried in at least a broadly similar fashion. Although the vertical pH gradient is mainly driven by the strength of the organic carbon pump, which may have varied temporally and spatially (Foster et al., 2012), the strength of our record lies again in the comparison of multiple core sites from different ocean basins. Therefore, as a first approximation the simple assumption was applied that the modern mean surface-to-depth pH gradient of –0.3 units, determined from the eWOCE Electronic Atlas of WOCE data (Schlitzer, 2000), remained constant over time. This approach is similar to the modeling study of Tyrrell and Zeebe (2004), who assumed a constant surface-to-depth $[CO_3^{2-}]$ gradient. Earth system and ocean carbon cycle models suggest that during the Eocene, i.e. the oldest part of our record, surface-ocean pH was approximately 0.32-0.45 units lower compared to today, depending on the geochemical model and its respective parameterization (Tyrrell and Zeebe, 2004; Ridgwell, 2005; Ridgwell and Schmidt, 2010). These numerical models in turn rely on assumptions of late Paleocene values of atmospheric pCO_2, which were set to as high as ~1000 (Tyrrell and Zeebe, 2004), 834 (Ridgwell and Schmidt, 2010) and ~750 ppmv (Ridgwell, 2005).

However, the 50-My pH history is very similar among the models, despite their different approaches. Ridgwell and Schmidt (2010) used the most recent proxy observations and modeled a PETM pH ~0.35 lower than today, thus supporting the Cenozoic surface-ocean pH increase modeled by Tyrrell and Zeebe (2004) and Ridgwell (2005). Although Ridgwell's (2005) model uses a suite of pCO_2-proxies that includes Pearson and Palmer's (2000) boron isotope data and thus contains a small element of circularity, Tyrrell and Zeebe (2004) used entirely independent pCO_2 estimates from the GEOCARB III model (Berner and Kothavala, 2001). Because the pH estimates of both models are nevertheless similar, and because Ridgwell's (2005) model also includes ample data from paleosols, stomata and alkenones (Royer et al., 2004), we used a near-linear increase in surface ocean pH of 0.39 since the last 50 My, which is intermediate between the two models (Fig. 1D), and subtracted 0.3 pH units from the surface ocean estimates to infer the concurrent change in deep-sea pH.

4. POTENTIAL SOURCES OF HIGH $\delta^{11}B_c$ FROM ODP SITE 1218

Boron isotope ratios derived from ODP 1218 show a fundamentally different picture than the other cores. A $\delta^{11}B_c$ minimum is observed at ~43 Ma, where $\delta^{11}B_c$ is comparable to the other cores, followed by a rise of approximately 5‰ until a maximum at 35 Ma before they decrease

until 25 Ma, where the data approach $\delta^{11}B_c$ of the other cores (Fig. 1C). The consistently higher $\delta^{11}B_c$ values measured in ODP 1218 suggest that this core site must have been influenced by regional variations in pH. We followed several lines of evidence to find an explanation for this observation, none of which appears to provide an entirely convincing interpretation for the higher $\delta^{11}B_c$ found in this core:

1) Today this location is at a water depth of 4.8 km, but the subsidence history suggests that 40 Ma ago it was located on the mid-ocean ridge at a much shallower depth of ~3 km (Fig. DR4A). At 34 Ma, the carbonate compensation depth (CCD) at this site deepened rapidly and extensively in two ~40,000-year long steps (Coxall et al., 2005). After ~40 Ma, this area thus may have seen a disproportionately higher $[CO_3^{2-}]$, respectively pH, than other oceans. The geochemical records from site 1218 show that $\delta^{18}O$, $\delta^{13}C$ and $\%CaCO_3$ are tightly coupled, suggesting that the reflected CCD-deepening and deep-ocean cooling are closely related to the onset of Antarctic glaciation (Coxall et al., 2005; Katz et al., 2011). This line of argument is supported by the concurrent increase in benthic foraminiferal Li/Ca, which has been interpreted as a significant increase in $[CO_3^{2-}]$ (Lear and Rosenthal, 2006). Our benthic $\delta^{11}B_c$ record shows similarities with the Li/Ca record (Lear and Rosenthal, 2006), indicating that boron isotope data from site 1218 are at least partially related to the CCD deepening and associated geochemical changes in the eastern equatorial Pacific (Fig. DR5). However, our record is of comparably low resolution and hence not capable to adequately resolve the Eocene/Oligocene Transition (EOT) similar to the Li/Ca record (Lear and Rosenthal, 2006). When calculating pH from this site using benthic $\delta^{11}B_c$ and $\delta^{11}B_{sw}$ inferred from our reconstruction, a ~0.7 pH unit increase is obtained between ~43 and 34 Ma, which exceeds the modeled surface ocean pH increase (Tyrrell and Zeebe, 2004; Ridgwell, 2005) at that time by ~0.2 units. Between ~38 und 34 Ma the inferred pH increase is approximately 0.3 units, which equals an increase in $[CO_3^{2-}]$ of ~70 µmol kg^{-1}, i.e. almost twice the rise estimated from Li/Ca (37 µmol kg^{-1} across the EOT) (Lear and Rosenthal, 2006). Therefore, our estimated pH values are considerably higher than suggested by independent estimates. The similarity of $\delta^{11}B_c$ with the Li/Ca record after 34 Ma and with the CCD history (van Andel, 1975) indicates that the boron isotope and Li/Ca records at site 1218 were governed by similar geochemical processes, where pH, respectively carbonate ion increase, went hand-in-hand with the CCD deepening in the eastern equatorial Pacific.

2) The observed $\delta^{11}B_c$ pattern may additionally or alternatively be influenced by changes in pore water, where $\delta^{11}B_{pw}$ is typically lower than in bottom water due to dissolution of opal and carbonates and B desorption from clays, all of which result in decreased $\delta^{11}B_{pw}$ (Rae et al., 2011). It is worth noting that ODP site 1218 is located on relatively young crustal material (~40 Ma), whereas the other cores used for this study were drilled on old (~70-145 Ma) aseismic ridges (Fig. DR1, Table DR1). The alteration of oceanic crust is an important sink for boron in

the ocean, where the lighter isotope ^{10}B is preferentially removed from seawater, resulting in an enrichment of $\delta^{11}B_{sw}$ (Smith et al., 1995). However, if ^{10}B removal by oceanic crust alteration exceeded ^{10}B enrichment by dissolution/desorption of low-$\delta^{11}B$ components in pore waters, the infaunal *O. umbonatus* and the shallow infaunal *C. mundulus* analyzed from this core may have been influenced by relatively higher porewater $\delta^{11}B$. While this argument seems reasonable for *O. umbonatus*, it would be a greater stretch for $\delta^{11}B_c$ measured in *C. mundulu*s, which typically calcifies close to bottom-water conditions.

It seems that none of the above processes alone can explain the large $\delta^{11}B_c$ deviations observed at ODP site 1218, but a combination of these processes is not unreasonable. Because other $\delta^{11}B_c$ data are consistent between core sites and ocean basins, and because site 1218 is the only one drilled on young oceanic crust, we excluded these data from the determination of mean ocean $\delta^{11}B_{sw}$.

FIGURES AND TABLES

Figure DR1. Bathymetric map showing modern locations of ODP/DSDP (black symbols) and surface sediment sites (white symbols) investigated in this study.

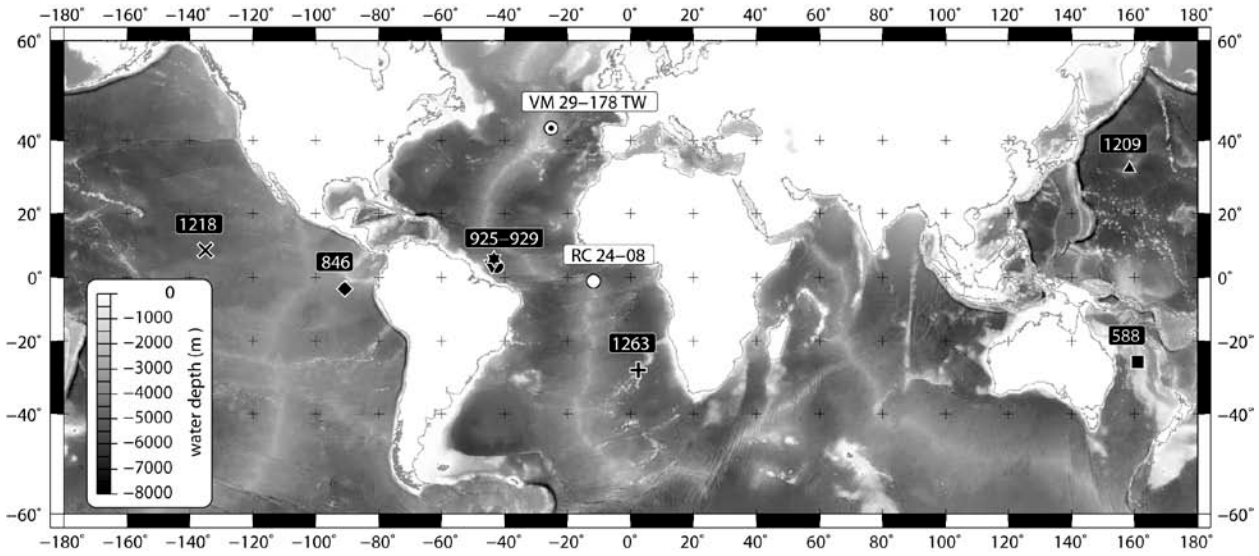

Figure DR2. Reconstructed deep-sea pH for the Atlantic (open symbols) and the Pacific (filled symbols) using benthic $\delta^{11}B_c$ and the apparent fractionation factor α_{app}=1.020 at **(A)** constant $\delta^{11}B_{sw}$ of 39.6‰, **(B)** variable $\delta^{11}B_{sw}$ estimated from geochemical modeling (Lemarchand et al., 2000), **(C)** variable $\delta^{11}B_{sw}$ estimated from the $\delta^{11}B_c$ differential between surface- and deep-dwelling planktic foraminifers (Pearson and Palmer, 2000), and **(D)** $\delta^{11}B$ of fluid inclusions in halites (Paris et al., 2010). Error bars reflect propagated ±2 s.e. Gray line and symbols are based on the same data, but were calculated using α=1.0272 (Klochko et al., 2006).

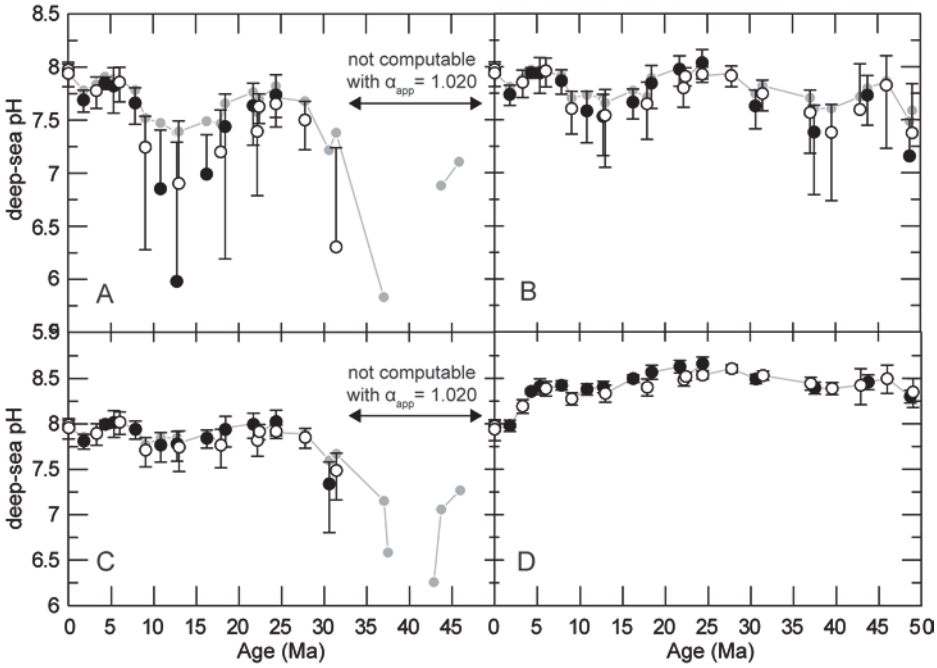

Figure DR3. Upper panel: $\delta^{11}B_c$ of the epibenthic *P. wuellerstorfi* and *C. mundulus* measured with NTIMS (yellow: Hönisch et al., 2008; red: this study) and MC-ICPMS (green: Rae et al., 2011) plotted against $\delta^{11}B$ of borate, the boron species preferentially incorporated into calcite. Error bars are 2 s.e. for TIMS and 2 s.d. for MC-ICPMS measurements. Data collected by NTIMS are consistently higher than data collected by MC-ICP-MS but systematic differences in the sensitivity to pH variations cannot be distinguished due to the relatively small pH range present in the deep ocean. **Lower panel:** Epibenthic $\delta^{11}B_c$ from Rae et al. (2011) compared to estimated bottom water $\delta^{11}B_{borate}$ values with 27.2‰ and 20‰ fractionation. The resulting regression lines are nearly identical.

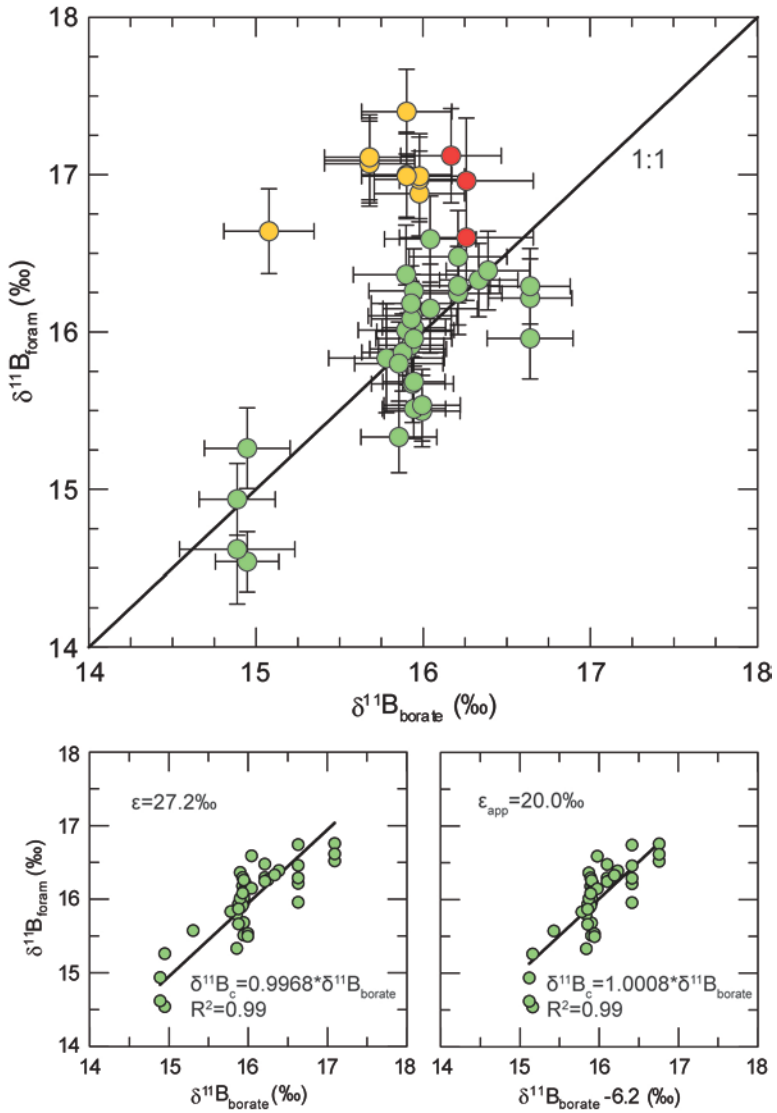

Figure DR4. (A) CCD history for different ocean basins from various studies: green=South Atlantic, blue=North Atlantic, red=average Pacific, yellow=equatorial Pacific (all from van Andel, 1975), black=equatorial Pacific (Lyle et al., 2010), brown=equatorial Pacific (Tripati et al., 2005). The thick gray line is the globally averaged and area-weighted CCD estimate (Lyle et al., 2008). Dashed lines are subsidence curves for three of the ODP sites studied here. All other sites are located well above the CCD. **(B)** $\delta^{11}B_c$ data normalized to *P. wuellerstorfi*. Numbers indicate analyzed subsamples of different species per data point, gray line represents 3-pt running average through data (excluding ODP 1218), and error bars reflect propagated 2 s.e. uncertainties.

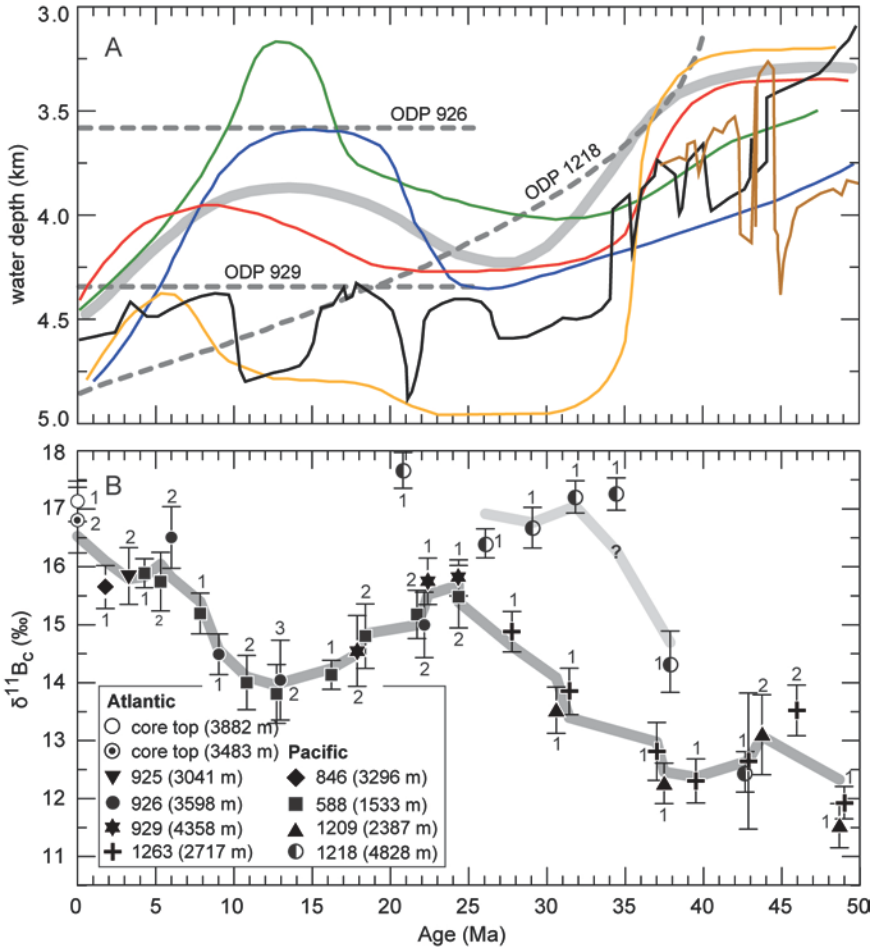

Figure DR5. Estimated pH from measured $\delta^{11}B_c$ at ODP site 1218, using secular $\delta^{11}B_{sw}$ as determined in this study (black symbols). Also plotted is the deep ocean pH inferred from averaged surface-ocean pH (Tyrrell and Zeebe, 2004; Ridgwell, 2005) (black line) and benthic foraminiferal Li/Ca (blue line), which is a calcite saturation proxy measured in the same core (Lear and Rosenthal, 2006). The gray bar indicates the time period when the equatorial Pacific CCD deepened by ~1.2 km (see Fig. DR4A).

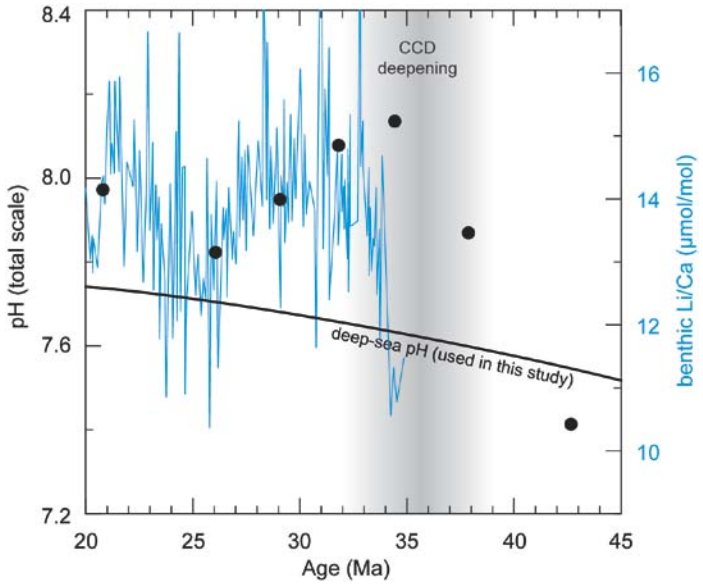

Table DR1.

ODP core information and sampling interval	Age (Ma)	paleo water depth (m)	pH (total scale) *	pKB	deep-sea temperature (°C) †	foraminiferal $\delta^{11}B$ (±2 external or internal s.e., whichever is larger)												average $\delta^{11}B$ normalized to *P. wuellerstorfi*	±2 s.e. (propagated error)
						P. wuellerstorfi			*C. mundulus*			*O. umbonatus*			*N. truempyi*				
						individual measurements §	average	±2 s.e.	individual measurements §	average	±2 s.e.	individual measurements §	average	±2 s.e.	individual measurements §	average	±2 s.e.		
ATLANTIC																			
Coretops (non ODP)																			
RC 24-08, 0-2 cm	3.8 ka	3882	7.93	8.67	2.0	17.08 16.51 17.18 17.26 17.69 16.99	17.12	0.35		—	—		—	—		—	—	17.12	0.35
VM 29-178 TW, 6-7 cm	3.8 ka	3483	7.96	8.69	2.4	16.51 16.68	16.60	0.47	16.97 16.95	16.96	0.47		—	—		—	—	16.81	0.70
Ceara Rise																			
154/925C/11H3/35-39 cm	3.28	3041	7.86	8.72	2.1	15.80 15.96 15.87 15.91 15.81 15.79	15.86	0.28	15.74 15.83	15.79	0.47		—	—		—	—	15.86	0.64
154/926C/17H3/97-101 cm	6.00	3598	7.85	8.67	3.8		—	—	16.33 16.05 16.04 16.28	16.18	0.35	15.34 15.54 15.03	15.30	0.40		—	—	16.48	0.90
154/926A/23H1/138-142 cm	9.03	3598	7.80	8.66	4.2		—	—	14.78 14.18 14.27 14.61	14.46	0.35		—	—		—	—	14.53	0.70
154/926A/28H3/6-10 cm	12.96	3598	7.76	8.65	5.6	14.59 14.30 14.82 14.61	14.76	0.35	14.24 13.97 13.78	14.00	0.40	12.21 11.93 12.64	12.06	0.44		—	—	14.15	1.00
154/929A/27X2/97-101 cm	17.87	4358	7.71	8.61	5.7		—	—	14.72 15.05 14.25	14.67	0.46	13.11 12.85 12.87	12.94	0.40		—	—	14.55	1.07
154/926B/45X3/41-45 cm	22.16	3598	7.71	8.64	5.9		—	—	14.99 15.43 14.44 14.36 15.37 15.43	15.00	0.40	13.49 12.90 13.31	13.23	0.40		—	—	14.86	0.83
154/929A/32X2/36-40 cm	22.38	4358	7.68	8.60	6.0		—	—	15.48 15.70 15.72	15.63	0.40		—	—		—	—	15.70	0.57
154/929A/36X4/36-40 cm	24.35	4358	7.66	8.60	6.5		—	—	16.11 15.77 15.59 15.60 15.76	15.77	0.31		—	—		—	—	15.84	0.51
Walvis Ridge																			
208/1263A/6H2/24-28 cm	27.76	2150	7.69	8.74	4.5		—	—	14.55 15.11 14.65 15.01	14.83	0.35		—	—		—	—	14.90	0.54
208/1263A/8H1/0-4 cm	31.42	2000	7.64	8.74	5.1		—	—	13.80 13.79 14.03	13.80	0.40		—	—		—	—	13.87	0.57
208/1263C/2H6/97-101 cm	37.01	1900	7.59	8.72	6.5		—	—		—	—	11.11 11.60	11.36	0.50		—	—	12.77	0.92
208/1263A/14H4/40-44 cm	39.51	1800	7.54	8.72	7.3		—	—		—	—	10.77 10.92 10.17 11.28	10.79	0.38		—	—	12.20	0.71
208/1263A/16H5/24-28 cm	42.86	1750	7.49	8.71	8.2		—	—		—	—	10.52 8.73 8.72 10.77	9.68	1.12	14.98 14.93 14.95 14.61	14.87	0.35	12.60	1.40

Table DR1 continued.

ODP core information and sampling interval	Age (Ma)	paleo water depth (m)	pH (total scale) *	pKB	deep-sea temperature (°C) †	foraminiferal $\delta^{11}B$ (±2 external or internal s.e., whichever is larger)												average $\delta^{11}B$ normalized to *P. wuellerstorfi*	±2 s.e. (propagated error)
						P. wuellerstorfi			*C. mundulus*			*O. umbonatus*			*N. truempyi*				
						individual measurements §	average	±2 s.e.	individual measurements §	average	±2 s.e.	individual measurements §	average	±2 s.e.	individual measurements §	average	±2 s.e.		
ATLANTIC																			
208/1263A/19H5/24-28 cm	45.95	1700	7.46	8.71	9.0		—	—		—	—	11.36 11.31 11.08 10.92 11.27	11.19	0.31	15.03 15.09 15.05 14.90 15.26	15.07	0.31	13.45	0.89
208/1263A/22H2/24-28 cm	48.98	1650	7.39	8.69	10.6		—	—		—	—		—	—	12.62 12.56 12.62 12.70 13.11 13.27	12.81	0.28	12.05	0.56
PACIFIC																			
138/846B/7H1/127-131 cm	1.78	3296	7.85	8.72	0.9	14.96 15.76 15.67 15.64	15.50	0.37		—	—		—	—		—	—	15.50	0.37
Lord Howe Rise																			
90/588/10H1/34-40 cm	4.28	1520	7.84	8.79	2.9	16.02 15.84 15.91 16.08 15.89 15.67 15.62	15.86	0.25		—	—		—	—		—	—	15.86	0.25
90/588/11H6/34-40 cm	5.31	1520	7.84	8.78	3.8		—	—	14.41 14.30 14.42 14.31 14.82	14.45	0.31	16.10 15.85 15.98	15.98	0.40		—	—	15.79	0.89
90/588/20H3/34-40 cm	7.84	1510	7.82	8.77	4.2		—	—	14.90 14.91 15.07 14.83	14.93	0.35		—	—		—	—	15.23	0.54
90/588/25H5/34-40 cm	10.81	1505	7.80	8.77	4.8	13.72 13.90 14.10 13.84	13.89	0.35	13.83 13.89 13.84 14.03 13.81	13.88	0.31		—	—		—	—	14.04	0.62
90/588A/5H3/32-37.5 cm	12.72	1500	7.79	8.76	5.5	14.04 13.94 13.94 14.06 13.90	13.97	0.31	13.34 13.42	13.38	0.40		—	—		—	—	13.83	0.65
90/588C/4R5/109-115 cm	16.22	1495	7.77	8.75	6.3		—	—	13.83 13.89 13.84 14.03 13.81	13.84	0.25		—	—		—	—	14.14	0.48
90/588C/2R3/109-115 cm	18.39	1490	7.76	8.76	5.7		—	—	14.82 14.74 15.04 15.22 15.36 15.26	15.08	0.28	12.73 13.38 13.51	13.21	0.48		—	—	14.71	0.92
90/588C/6R7/34-40 cm	21.69	1485	7.73	8.76	5.5		—	—	15.54 15.17 15.00 14.67 15.57 15.24	15.20	0.28	13.84 14.05 14.35 14.22 13.84	14.06	0.31		—	—	15.20	0.84
90/588C/9R6/109-115 cm	24.35	1480	7.71	8.75	6.5		—	—	14.80 15.28 15.72 15.76 15.16	15.35	0.36	14.58 14.84 14.59	14.67	0.40		—	—	15.58	0.91

Table DR1 continued.

ODP core information and sampling interval	Age (Ma)	paleo water depth (m)	pH (total scale) *	pKB	deep-sea temperature (°C) †	foraminiferal $\delta^{11}B$ (±2 external or internal s.e., whichever is larger)									average $\delta^{11}B$ normalized to *P. wuellerstorfi*	±2 s.e. (propagated error)
						P. wuellerstorfi			*C. mundulus*			*O. umbonatus*			*N. truempyi*				
						individual measurements §	average	±2 s.e.	individual measurements §	average	±2 s.e.	individual measurements §	average	±2 s.e.	individual measurements §	average	±2 s.e.		
PACIFIC																			
Shatsky Rise																			
198/1209A/13H3/52-56 cm	30.59	2150	7.53	8.73	4.8		——	——	13.12 13.43 13.23	13.23	0.40		——	——		——	——	13.53	0.57
198/1209B/16H3/37-44 cm	37.48	2050	7.44	8.72	6.6		——	——		——	——	11.64 11.27 11.18 11.83	11.46	0.35		——	——	12.30	0.70
198/1209A/16H5/48-54 cm	43.73	2000	7.37	8.70	8.2		——	——		——	——	11.53 12.30 12.71	12.30	0.69		——	——	13.14	0.92
198/1209A/18H4/38-44 cm	48.68	1950	7.30	8.68	10.4		——	——		——	——	11.54 10.73 11.18 10.53 10.68	10.93	0.38		——	——	11.78	0.71
Abyssal ODP Site 1218																			
199/1218B/8H4/23-25 cm	20.80	4300	7.74	8.61	5.3		——	——	17.37 16.94 17.43 17.74 17.03	17.30	0.31		——	——		——	——	17.61	0.51
199/1218B/13H6/56-62 cm	26.06	4100	7.72	8.63	5.3		——	——	16.22 16.46 16.11 16.41 15.85 16.02 15.70	16.11	0.25		——	——		——	——	16.41	0.48
199/1218C/11H3/100-104 cm	29.07	4000	7.71	8.64	4.6		——	——	16.26 16.57 16.51 16.08	16.35	0.35		——	——		——	——	16.66	0.54
199/1218C/15X2/135-139 cm	31.81	3800	7.68	8.64	5.1		——	——	16.79 16.66 16.95 16.88 17.16 17.01	16.91	0.28		——	——		——	——	17.21	0.50
199/1218B/24X4/40-46 cm	34.43	3700	7.67	8.64	6.2		——	——	17.18 16.60 17.07 17.10 16.85 16.41	16.87	0.28		——	——		——	——	17.17	0.50
199/1218B/26X4/23-31 cm	37.87	3450	7.64	8.64	6.7		——	——		——	——	13.56 14.14 13.15	13.62	0.53		——	——	14.46	0.80
199/1218A/30X2/125-135 cm	42.66	2700	7.61	8.66	8.2		——	——		——	——	11.55 11.91 11.76 11.17	11.48	0.35		——	——	12.32	0.70

***** **Averaged surface-ocean pH (Tyrrell and Zeebe, 2004; Ridgwell, 2005) – 0.3 pH units**

† **according to van Tuyll et al. (2007)**

§ **only acceptable runs with mass fractionation <1‰**

REFERENCES CITED

van Andel, T.H., 1975, Mesozoic/cenozoic calcite compensation depth and the global distribution of calcareous sediments: Earth and Planetary Science Letters, v. 26, no. 2, p. 187-194, doi: 10.1016/0012-821X(75)90086-2.

Barker, S., Greaves, M., and Elderfield, H., 2003, A study of cleaning procedures used for foraminiferal Mg/Ca paleothermometry: Geochemistry Geophysics Geosystems, v. 4, no. 9, 8407, doi: 10.1029/2003GC000559.

Berner, R.A., and Kothavala, Z., 2001, Geocarb III: A Revised Model of Atmospheric CO_2 over Phanerozoic Time: American Journal of Science, v. 301, no. 2, p. 182–204, doi: 10.2475/ajs.301.2.182.

Coxall, H.K., Wilson, P.A., Palike, H., Lear, C.H., and Backman, J., 2005, Rapid stepwise onset of Antarctic glaciation and deeper calcite compensation in the Pacific Ocean: Nature, v. 433, no. 7021, p. 53–57, doi: 10.1038/nature03135.

Foster, G.L., Lear, C.H., and Rae, J.W.B., 2012, The evolution of pCO_2, ice volume and climate during the middle Miocene: Earth and Planetary Science Letters, v. 341–344, p. 243–254, doi: 10.1016/j.epsl.2012.06.007.

Foster, G.L., Pogge von Strandmann, P.A.E., and Rae, J.W.B., 2010, Boron and magnesium isotopic composition of seawater: Geochemistry Geophysics Geosystems, v. 11, Q08015, doi: 10.1029/2010GC003201.

Hemming, N.G., and Hanson, G.N., 1992, Boron isotopic composition and concentration in modern marine carbonates: Geochimica et Cosmochimica Acta, v. 56, no. 1, p. 537-543, doi: 10.1016/0016-7037(92)90151-8.

Hönisch, B., Bickert, T., and Hemming, N.G., 2008, Modern and Pleistocene boron isotope composition of the benthic foraminifer *Cibicidoides wuellerstorfi*: Earth and Planetary Science Letters, v. 272, no. 1-2, p. 309-318, doi: 10.1016/j.epsl.2008.04.047.

Hönisch, B., Hemming, N.G., and Loose, B., 2007, Comment on "'A critical evaluation of the boron isotope-pH proxy: The accuracy of ancient ocean pH estimates'" by M. Pagani, D. Lemarchand, A. Spivack and J. Gaillardet: Geochimica et Cosmochimica Acta, v. 71, no. 6, p. 1636-1641, doi: 10.1016/j.gca.2006.07.045.

Katz, M.E., Cramer, B.S., Toggweiler, J.R., Esmay, G., Liu, C., Miller, K.G., Rosenthal, Y., Wade, B.S., and Wright, J.D., 2011, Impact of Antarctic Circumpolar Current Development on Late Paleogene Ocean Structure: Science, v. 332, no. 6033, p. 1076 - 1079, doi: 10.1126/science.1202122.

Klochko, K., Kaufman, A.J., Yao, W., Byrne, R.H., and Tossell, J.A., 2006, Experimental measurement of boron isotope fractionation in seawater: Earth and Planetary Science Letters, v. 248, p. 276-285, doi: 10.1016/j.epsl.2006.05.034.

Krief, S., Hendy, E.J., Fine, M., Yam, R., Meibom, A., Foster, G.L., and Shemesh, A., 2010, Physiological and isotopic responses of scleractinian corals to ocean acidification: Geochimica et Cosmochimica Acta, v. 74, no. 17, p. 4988-5001, doi: 10.1016/j.gca.2010.05.023.

Lear, C.H., and Rosenthal, Y., 2006, Benthic foraminiferal Li/Ca: Insights into Cenozoic seawater carbonate saturation state: Geology, v. 34, no. 11, p. 985-988, doi: 10.1130/G22792A.1.

Lear, C.H., Elderfield, H., and Wilson, P.A., 2000, Cenozoic deep-sea temperatures and global ice volumes from Mg/Ca in benthic foraminiferal calcite: Science, v. 287, no. 5451, p. 269-272, doi: 10.1126/science.287.5451.269.

Lemarchand, D., Gaillardet, J., Lewin, É., and Allègre, C.J., 2000, The influence of rivers on marine boron isotopes and implications for reconstructing past ocean pH: Nature, v. 408, p. 951-954, doi: 10.1038/35050058.

Lutze, G.F., and Thiel, H., 1989, Epibenthic foraminifera from elevated microhabitats: *Cibicidoides wuellerstorfi* and *Planulina ariminensis*: Journal of Foraminiferal Research, v. 19, p. 153-158, doi: 10.2113/gsjfr.19.2.153.

Lyle, M., Barron, J., Bralower, T.J., Huber, M., Lyle, A.O., Ravelo, A.C., Rea, D.K., and Wilson, P.A., 2008, Pacific ocean and Cenozoic evolution of climate: Reviews of Geophysics, v. 46, p. 1–47, doi: 10.1029/2005RG000190.

Lyle, M., Pälike, H., Nishi, H., Raffi, I., Gamage, K., Klaus, A., and IODP Expeditions 320/321 Scientific Party, 2010, The Pacific Equatorial Age Transect, IODP Expeditions 320 and 321: Building a 50-Million-Year-Long Environmental Record of the Equatorial Pacific Ocean. Scientific Drilling: v. 9, p. 4–15, doi: 10.2204/iodp.sd.9.01.2010.

Paris, G., Gaillardet, J., and Louvat, P., 2010, Geological evolution of seawater boron isotopic composition recorded in evaporites: Geology, v. 38, no. 11, p. 1035-1038, doi: 10.1130/G31321.1.

Pearson, P.N., and Palmer, M.R., 2000, Atmospheric carbon dioxide concentrations over the past 60 million years: Nature, v. 406, p. 695-699, doi: 10.1038/35021000.

Rae, J.W.B., Foster, G.L., Schmidt, D.N., and Elliott, T., 2011, Boron isotopes and B/Ca in benthic foraminifera: Proxies for the deep ocean carbonate system: Earth and Planetary Science Letters, v. 302, no. 3-4, p. 403-413, doi: 10.1016/j.epsl.2010.12.034.

Raitzsch, M., Kuhnert, H., Hathorne, E.C., Groeneveld, J., and Bickert, T., 2011, U/Ca in benthic foraminifers: A proxy for the deep-sea carbonate saturation: Geochemistry Geophysics Geosystems, v. 12, no. 6, Q06019, doi: 10.1029/2010GC003344.

Rathburn, A.E., and Corliss, B.H., 1994, The ecology of living (stained) deep-sea benthic foraminifera from the Sulu Sea: Paleoceanography, v. 9, no. 1, p. 87-150, doi: 10.1029/93PA02327.

Ridgwell, A., 2005, A Mid Mesozoic Revolution in the regulation of ocean chemistry: Marine Geology, v. 217, no. 3-4, p. 339-357, doi: 16/j.margeo.2004.10.036.

Ridgwell, A., and Schmidt, D.N., 2010, Past constraints on the vulnerability of marine calcifiers to massive carbon dioxide release: Nature Geoscience, v. 3, no. 3, p. 196-200, doi: 10.1038/ngeo755.

Rollion-Bard, C., and Erez, J., 2010, Intra-shell boron isotope ratios in the symbiont-bearing benthic foraminiferan *Amphistegina lobifera*: Implications for $\delta^{11}B$ vital effects and paleo-pH reconstructions: Geochimica et Cosmochimica Acta, v. 74, no. 5, p. 1530–1536, doi: 10.1016/j.gca.2009.11.017.

Royer, D.L., Berner, R.A., Montañez, I.P., Tabor, N.J., and Beerling, D.J., 2004, CO_2 as a primary driver of Phanerozoic climate: GSA Today, v. 14, no. 3, p. 4, doi: 10.1130/1052-5173(2004)014<4:CAAPDO>2.0.CO;2.

Schlitzer, R., 2000, Electronic Atlas of WOCE Hydrographic and Tracer Data Now Available: EOS, Transactions American Geophysical Union, v. 81, no. 5, p. 45, doi: 10.1029/00EO00028.

Smith, H.J., Spivack, A.J., Staudigel, H., and Hart, S.R., 1995, The boron isotopic composition of altered oceanic crust: Chemical Geology, v. 126, no. 2, p. 119-135, doi: 10.1016/0009-2541(95)00113-6.

Tripati, A., Backman, J., Elderfield, H., and Ferretti, P., 2005, Eocene bipolar glaciation associated with global carbon cycle changes: Nature, v. 436, no. 7049, p. 341–346, doi: 10.1038/nature03874.

van Tuyll, C.I., van de Wal, R.S.W., and Oerlemans, J., 2007, The response of a simple Antarctic ice-flow model to temperature and sea-level fluctuations over the Cenozoic era: Annals of Glaciology, v. 46, no. 1, p. 69-77, doi: 10.3189/172756407782871413.

Tyrrell, T., and Zeebe, R.E., 2004, History of carbonate ion concentration over the last 100 million years: Geochimica et Cosmochimica Acta, v. 68, no. 17, p. 3521-3530, doi: 10.1016/j.gca.2004.02.018.

Zachos, J., Pagani, M., Sloan, L., Thomas, E., and Billups, K., 2001, Trends, Rhythms, and Aberrations in Global Climate 65 Ma to Present: Science, v. 292, no. 5517, p. 686-693, doi: 10.1126/science.1059412.